Fish and Shellfish Immunology 94 (2019) 271–279

Contents lists available at ScienceDirect

Fish and Shellfish Immunology

journal homepage: www.elsevier.com/locate/fsi

Full length article

Effect of vitamin D3 on immunity and antioxidant capacity of pearl oyster *Pinctada fucata martensii* after transplantation: Insights from LC–MS-based metabolomics analysis

Chuangye Yang[a,b], Xiaodong Du[a,b,**], Ruijuan Hao[a], Qingheng Wang[a,b], Yuewen Deng[a,b,*], Ruijiao Sun[c]

[a] Fisheries College, Guangdong Ocean University, Zhanjiang, 524088, China
[b] Pearl Breeding and Processing Engineering Technology Research Centre of Guangdong Province, Zhanjiang, 524088, China
[c] Zhejiang Hengxing Food Co., Ltd, Jiaxing, 314100, China

ARTICLE INFO

Keywords:
Pinctada fucata martensii
Liquid chromatography–mass spectrometry (LC–MS)
Vitamin D3
Metabolomics

ABSTRACT

Postoperative care is a critical step of pearl culture that ultimately determines culture success. To determine the effect of dietary vitamin D3 (VD3) levels on immunity and antioxidant capacity of pearl oyster *Pinctada fucata martensii* during postoperative care and explore the mechanisms behind this phenomenon, five isonitrogenous and isolipidic experimental diets were formulated by adding different levels of dietary VD3 (0, 500, 1000, 3000, and 10000 IU/kg), and the diets were fed to five experimental groups (EG1, EG2, EG3, EG4, and EG5) in turn and cultured indoors. The control group (CG) was cultured in the natural sea. Pearl oysters that were 1.5 years old were subjected to nucleus insertion. After culturing for 30 days, EG3 exhibited significantly higher survival rates than those in CG and EG5 ($P < 0.05$). Moreover, EG3 exhibited the highest activities of alkaline phosphatase, acid phosphatase, catalase, superoxide dismutase, and lysozyme. However, EG5 achieved the highest activities of glutathione peroxidase. Metabolomics-based profiling of pearl oysters fed with high levels of dietary VD3 (EG5) and optimum levels of dietary VD3 (EG3) revealed 76 significantly differential metabolites (SDMs) (VIP > 1 and $P < 0.05$). Pathway analysis indicated that SDMs were involved in 21 pathways. Furthermore, integrated key metabolic pathway analysis suggested that pearl oysters in EG5 regulated the pentose phosphate pathway, glutathione metabolism, sphingolipid metabolism, and arachidonic acid metabolism in response to stress generated from excessive VD3. These findings had significant implications on strengthening the future development and application of VD3 in aquaculture of pearl oyster *P. f. martensii*.

1. Introduction

The pearl oyster *Pinctada fucata martensii* is a filter feeder animal and well known throughout the world for its ability to produce high-quality pearls; this oyster accounts for more than 90% of seawater pearl production [1]. In pearl farming, the process of pearl culture are as follows: 1) preoperative conditioning, 2) implantation of a nucleus and epithelial cells of mantle grafts, 3) postoperative care, and 4) culturing and harvest [1]. Among these steps, postoperative care ensures that host oysters heal in small mesh nets under stable environmental conditions after implantation, while the graft tissue firmly clings to the gonad tissue with the proliferation of epithelial cells and forms a pearl sac that envelops the nucleus [2]. The pearl is then formed from the deposition of nacre around the nucleus. However, a strong response can lead to nucleus rejection, failure of pearl sac formation, and death of the host oyster. Therefore, postoperative care is a critical step of pearl culture that ultimately determines culture success. Hence, many studies on pearl culture have focused on methodologies to improve the success of postoperative care [3–5]. For example, Atsumi et al. [3] proposed a new postoperative care method in which pearl oysters were immersed in low-salinity seawater to increase the production of high-quality pearls. Although our research team also demonstrated that culturing pearl oyster indoors by using formulated diets could improve pearl production [6], our knowledge on the roles of specific nutrients in improving pearl oyster immunity during the postoperative care period and the underlying mechanisms in oyster species remains limited.

* Corresponding author. Fisheries College, Guangdong Ocean University, Zhanjiang, 524088, China.
** Corresponding author. Fisheries College, Guangdong Ocean University, Zhanjiang, 524088, China.
E-mail addresses: gdhddxd@hotmail.com (X. Du), dengyw@gdou.edu.cn (Y. Deng).

https://doi.org/10.1016/j.fsi.2019.09.017
Received 4 June 2019; Received in revised form 31 August 2019; Accepted 5 September 2019
Available online 06 September 2019

Vitamin D (VD) is classified as a secosteroid involved in the physiological functions of animals; it plays not only an important role in calcium and phosphorus metabolism and bone development but also influences the immune function of aquatic animals [7]. Thus, VD is an essential nutrient required for the normal growth of aquatic animals [8]. However, excess vitamin D3 (VD3) could cause metabolic disturbances in or stress to aquatic animals [9,10]. Therefore, optimum levels of VD3 in the diet must be carefully evaluated and determined, especially for unstudied species.

As an emerging technological and analytical approach, metabolomics could be used to measure large numbers of low-molecular weight quantitatively by using a high-throughput approach [11], such as gas chromatography–mass spectrometry [12–14], liquid chromatography–mass spectrometry (LC–MS) [15,16], and nuclear magnetic resonance [17,18]. This potential has been explored to assess the effects of food shortage [19,20], nutrient supplementation [21], differences in nutrient levels [22,23], and dietary protein or lipid substitution [24,25] in aquatic animals via metabolomics approaches.

Considering all these circumstances, different dietary levels of VD3 were fed to pearl oyster *P. f. martensii* by using land-based culture after implantation, and LC–MS-based metabolomics was performed and combined with multivariate analyses to evaluate the effect of high doses of VD3 on the pearl oyster during postoperative care. The results further contribute to understanding the underlying mechanisms of VD3 in the modulation of pearl oyster metabolic profiles and promote the development of *P. f. martensii* aquaculture.

2. Materials and methods

2.1. Experimental diet and procedures

Five isonitrogenous and isolipidic experimental diets were formulated, in which different levels of dietary VD3 (0, 500, 1000, 3000, and 10000 IU/kg) were added based on our previous studies [25–28]. These diets were stored at −20 °C until use.

Experiments were conducted from October to November 2018. The fifth-generation selected line for faster growth was used in the experiment. The selected line was designated as “Haixuan NO 1,” and the line development was described in detail by Du et al. [29]. Pearl oysters that were 1.5 years old with a mean shell length of 60.35 ± 6.11 mm were chosen and subjected to nucleus insertion. In surgery, a small piece of mantle tissue (approximately 4 mm^2) from a donor oyster and a small (5.5 mm in diameter) nucleus were implanted into the gonad of the host oyster in accordance with conventional methods [30]. These animals were randomly assigned to five experimental groups (EG1, EG2, EG3, EG4, and EG5) and one control group (CG). CG was cultured in the natural sea of Liusha Bay in Guangdong, China. Experimental groups were cultured indoors, and three tanks were prepared for each group. Each tank had 7 net cages, and 30 animals were assigned to each cage. The volume of water was 1000 L. Diet doses were specified based on a previous study [31]; the pearl oysters were fed every 4 h. Water was replaced at a volume of 300 L daily. The experimental period lasted for 30 days, and the following water parameters were maintained: dissolved oxygen at 5.00 mg/L, temperature at 27.1 °C–29.0 °C, and salinity at 30‰.

2.2. Sample collection

After culturing for 30 days, the total number of pearl oysters in each replicate was measured to calculate the survival rate during postoperative care. Survival rates were calculated in accordance with the methods described by Yang et al. [26]. Hepatopancreatic tissues from each animal were dissected, immediately placed in liquid nitrogen, and then stored at −80 °C until analysis.

2.3. Biochemical assays

Six hepatopancreatic tissues were collected from each replicate for biochemical measurements. Tissues were homogenized, and homogenates were centrifuged (10,000 × *g* for 20 min at 4 °C) by using a high-speed refrigerated centrifuge. The supernatant solution was transferred to new 2.0 mL tubes. Protein contents of samples were measured by using Folin's method with bovine serum albumin as the standard. Alkaline phosphatase (AKP), acid phosphatase (ACP), catalase (CAT), superoxide dismutase (SOD), glutathione peroxidase (GPx), and lysozyme (LYS) were also determined via commercial kits (Beijing Dongge Weiye Technology Co., Ltd.; Beijing, China) according to the manufacturer's instructions. All assays were conducted within 24 h after extraction.

2.4. Metabolite extraction

On the basis of immunity and antioxidant capacities of pearl oysters, we compared the metabolic profiles of pearl oysters with high levels of dietary VD3 with those with optimum levels of dietary VD3. A sample (50 mg) was obtained and placed in the EP tube. Then, 1000 μL of extraction solvent containing the internal target (V methanol: V acetonitrile: V water = 2:2:1, containing internal standard 2 μg/mL) was added. The solution was homogenized in a ball mill for 4 min at 45 Hz and then ultrasound-treated for 5 min (incubated in ice water). After three rounds of homogenization, the solution was incubated for 1 h at −20 °C to precipitate proteins and subsequently centrifuged at 12,000 rpm for 15 min at 4 °C. The supernatant (825 μL) was transferred fresh into EP tubes, extracts were dried in a vacuum concentrator without heating, and 200 μL extraction solvent (V acetonitrile: V water = 1:1) was added for reconstitution. Vortexing for 30 s and sonicating for 10 min (4 °C water bath) was conducted, followed by centrifuging for 15 min at 12,000 rpm and 4 °C. The supernatant (75 μL) was transferred into a fresh 2 mL LC/MS glass vial, and 10 μL was obtained from each sample and pooled as quality control (QC) samples. Then, 75 μL of supernatant was obtained for UHPLC–QTOF–MS analysis.

2.5. LC–MS/MS analysis

LC–MS/MS analyses were conducted by using a UHPLC system (1290, Agilent Technologies) with a UPLC BEH Amide column (1.7 μm 2.1 mm × 100 mm, Waters) coupled with Triple TOF 6600 (Q-TOF, AB Sciex). The mobile phase consisted of (A) 25 mM of NH_4Ac and 25 mM of NH_4OH in water (pH = 9.75) (B) and acetonitrile that was carried with the following elution gradient: 0 min, 95% B; 0.5 min, 95% B; 7 min, 65% B; 8 min, 40% B; 9 min, 40% B; 9.1 min, 95% B; 12 min, and 95% B, which was delivered in 0.5 mL min^{-1}. The injection volume was 1 μL. The Triple TOF mass spectrometer was used to obtain MS/MS spectra on an information-dependent basis (IDA) during an LC/MS experiment. In this mode, the acquisition software (Analyst TF 1.7, AB Sciex) continuously evaluated the full-scan survey MS data as it collected and triggered the acquisition of MS/MS spectra depending on preselected criteria. In each cycle, 12 precursor ions with intensities greater than 100 were chosen for fragmentation at the collision energy of 30 V (15 MS/MS events with a product ion accumulation time of 50 msec each). ESI source conditions were set as follows: ion source gas 1 at 60 Psi, ion source gas 2 at 60 Psi, curtain gas at 35 Psi, source temperature at 600 °C, and ion spray voltage floating at 5000 or −4000 V in positive or negative modes, respectively.

2.6. Data analysis

MS raw data (.wiff) files were converted to the mzXML format via ProteoWizard (http://proteowizard.sourceforge.net/downloads.shtml) and processed by using R package XCMS (version 3.2). The

preprocessing results generated a data matrix that consisted of retention time (RT), mass-to-charge ratio values, and peak intensity. R package CAMERA was used for peak annotation after XCMS data processing. In-house MS2 database was applied for metabolite identification [32,33].

The resultant three-dimensional data involving the peak number, sample name, and normalized peak area were fed to a SIMCA software package (v14.1; Sartorius Stedim Data Analytics AB; Umea, Sweden) for principal component analysis (PCA) and orthogonal projections to latent structures–discriminate analysis (OPLS–DA). PCA showed the distribution of origin data. To obtain an enhanced level of group separation and obtain an increased understanding of variables responsible for classification, supervised OPLS–DA was applied. Moreover, sevenfold cross validation was used to estimate the robustness and predictive ability of our model. This permutation test was conducted to validate the model further. On the basis of OPLS–DA, a loading plot was constructed showing the contribution of variables to differences between the two groups. To refine this analysis, the first principal component of variable importance in the projection (VIP) was obtained. If $P < 0.05$ and VIP > 1, then the variable was defined as a significantly differential metabolite (SDM) between the groups [34]. In addition, commercial databases, including KEGG (http://www.genome.jp/kegg/) and MetaboAnalyst (http://www.metaboanalyst.ca/) were utilized to search for metabolite pathways.

The results of the survival rate and biochemical data were expressed as mean ± SEM, and the significant differences ($P < 0.05$) among variables were determined by using one-way ANOVA and Tukey's method. All analyses were conducted via IBM SPSS Statistics 19 (IBM, USA).

3. Results

3.1. Survival rate

At the end of the experiment, survival rates of pearl oysters ranged from 79.70% to 88.49%. The pearl oysters in EG3 exhibited significantly higher survival rates than those in CG and EG5 ($P < 0.05$, Fig. 1).

3.2. Activities of immune- and antioxidant-related enzymes

Table 1 lists the responses of immune- and antioxidant-related enzymes (AKP, ACP, SOD, CAT, GPx, and LYS) in the hepatopancreas of pearl oysters in the experimental and control groups. EG3 exhibited the highest activities of AKP, ACP, SOD, CAT, and LYS. AKP and CAT activities were significantly higher in EG3 than those in CG, EG4, and EG5 ($P < 0.05$). EG3 indicated significantly higher ACP activities than EG4 and CG ($P < 0.05$). SOD and LYS activities in EG3 were significantly higher than those in other groups ($P < 0.05$). However, EG5 achieved the highest activities of GPx, which was significantly higher than those of other groups ($P < 0.05$).

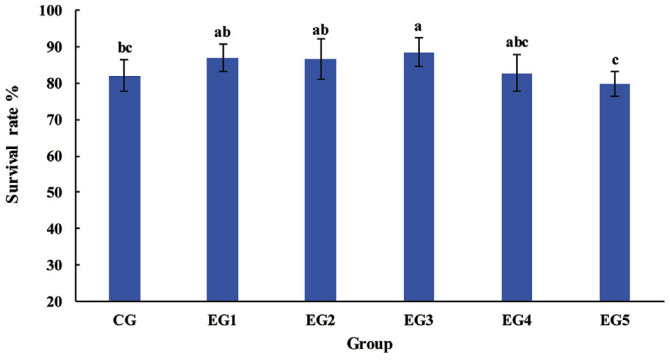

Fig. 1. Survival rates of pearl oyster *P. f. martensii* in experimental and control groups. Means with the same letters are not significantly different ($P > 0.05$).

3.3. Identification and quantification of LC–MS compounds

The ionization source of LC–QTOF/MS was electrospray ionization, including positive (POS) and negative (NEG) ion modes. QC samples were analyzed to detect the stability and repeatability of the system. The peak RT and peak area of total ion chromatograms (TICs) from all QC samples overlapped well, thereby indicating that the analytical system was stable (Supplementary Fig. 1). A total of 2385 and 2246 valid peaks were identified in POS and NEG for the hepatopancreas of the pearl oyster, respectively. On the basis of the in-house MS2 database, these valid peaks were matched for 487 (POS) and 287 (NEG) metabolites.

3.4. Multivariate analysis of metabolites

Given that PCA is an unsupervised pattern recognition method, it can reveal the intrinsic variations within data and reduce data dimensionality. In the PCA score scatter plot, similar datasets were clustered more closely, whereas different datasets were placed further apart. Fig. 2(A) and (B) illustrate the PCA results of UHPLC–QTOF/MS metabolic profiles. R^2X value of the PCA model between EG5 and EG3 was 0.556 (POS) and 0.531 (NEG). All samples in each score scatter plot were within the 95% Hotelling's T-squared ellipse. Based on these results, the metabolic datasets warranted further analysis.

To maximize the discrimination between the two groups, OPLS–DA was used to explain the different metabolic patterns. Fig. 2(C) and (D) show the OPLS–DA results for the hepatopancreas of the pearl oyster. All samples in each score scatter plot of the OPLS–DA model were inside the 95% Hotelling's T-squared ellipse. R^2X, R^2Y, and Q^2 values of the OPLS–DA model of POS and NEG between EG5 and EG3 were 0.366, 0.928, and 0.440, respectively. R^2X, R2Y, and Q2 value of the OPLS–DA model of NEG between EG5 and EG3 were 0.445, 0.897, and 0.496, respectively. To avoid the transition fit of the OPLS–DA mode, the permutation test was used for verification. Fig. 2(E) and (F) and present the results. The permutation test results for the R^2Y and Q^2 intercepts were 0.89 and −0.53 between EG5 and EG3 (POS) and 0.82 and −0.66 between EG5 and EG3 (NEG), respectively. The results indicated that the OPLS–DA model had no overfitting and good stability, making it suitable for optimization in subsequent analyses.

3.5. Significantly differential metabolites

According to the principle that the P value of the *t*-test was < 0.05 and the VIP of the OPLS–DA model was > 1, SDMs were screened from all identified metabolites. Fig. 3(A) and (B) illustrate the volcano plots of SDMs. The figures clearly show that many metabolites were significantly different. Seventy-six SDMs were obtained between group EG5 and EG3 (POS: 50, NEG: 26) (Figs. 4 and 5, Supplementary Table 1). Compared with EG5, 22 SDMs had higher concentrations in EG3.

3.6. Metabolic pathway analysis of significantly differential metabolites

To explore the potential metabolic pathways affected by different dietary VD3 levels, SDMs were imported into MetaboAnalyst 4.0. The bubble plots in Fig. 6(A) and (B) demonstrate the main influential metabolic pathways in which the SDMs in the hepatopancreas are involved. Twenty-one metabolic pathways were found between groups EG5 and EG3 (POS: 9, NEG: 12) (Supplementary Table 2). On the basis of both –ln *P*-value and pathway impact scores, the relevant metabolic pathways were identified as glutathione metabolism, histidine metabolism, sphingolipid metabolism, tryptophan metabolism, and pyrimidine metabolism in POS between groups EG5 and EG3. The relevant metabolic pathways were identified as pentose phosphate pathway,

Table 1
Activities of immune-related enzymes of *P. f. martensii* in the experimental and control groups.

Group	AKP (IU/g prot)	ACP (IU/g prot)	SOD (IU/mg prot)	CAT (U/mg prot)	GPx (U/mg prot)	LYS (U/g prot)
CG	5.44 ± 0.64 b	1.04 ± 0.09 b	48.42 ± 5.49 bc	10.72 ± 1.56 b	3.57 ± 0.61 c	1.35 ± 0.23 b
EG1	6.47 ± 1.01 ab	1.30 ± 0.34 ab	58.69 ± 8.34 b	15.08 ± 2.67 ab	4.44 ± 0.34 bc	1.91 ± 0.19 b
EG2	7.19 ± 1.64 ab	1.34 ± 0.26 ab	54.09 ± 4.99 bc	15.14 ± 3.34 ab	4.43 ± 0.49 bc	1.60 ± 0.28 b
EG3	9.35 ± 1.99 a	1.81 ± 0.34 a	79.93 ± 12.61 a	18.51 ± 4.32 a	4.63 ± 0.46 b	2.25 ± 0.24 a
EG4	5.38 ± 1.07 b	0.98 ± 0.21 b	43.01 ± 7.87 c	9.71 ± 2.37 b	4.69 ± 0.19 b	1.15 ± 0.33 b
EG5	6.27 ± 0.91 b	1.25 ± 0.23 ab	57.23 ± 6.97 b	11.53 ± 2.21 b	5.66 ± 0.39 a	1.53 ± 0.26 b

AKP, alkaline phosphatase; ACP, acid phosphatase; SOD, superoxide dismutase, CAT, catalase; GPx, glutathione peroxidase; LYS: lysozyme.
Within the column, means with the same letters are not significant different ($P > 0.05$).

propanoate metabolism, ubiquinone and other terpenoid–quinone biosynthesis, citrate cycle, amino sugar and nucleotide sugar metabolism, glutathione metabolism, and tyrosine metabolism in NEG between groups EG5 and EG3.

4. Discussion

Increase in cultured pearl yield and quality is essential to pearl farm viability and a remarkable challenge in research and development. Nucleus implantation can cause serious trauma on host oysters, and improper postoperative care can lead to a large number of host oyster deaths, thereby affecting the yield and quality of pearls [3]. Therefore, the purpose of postoperative care is to restore the health of the host oyster, prevent death, and more importantly, rest the nucleus and avoid movement before the pearl sac is formed. Hence, denucleation and the occurrence of deformed beads are prevented. However, pearl oysters suspended from the raft in the sea throughout the postoperative care period were susceptible to a variable environment (e.g., salinity, temperature, environmental pollution, biofouling, pathogenic microorganisms, and phytoplankton biomass) [35–37]. These disadvantages

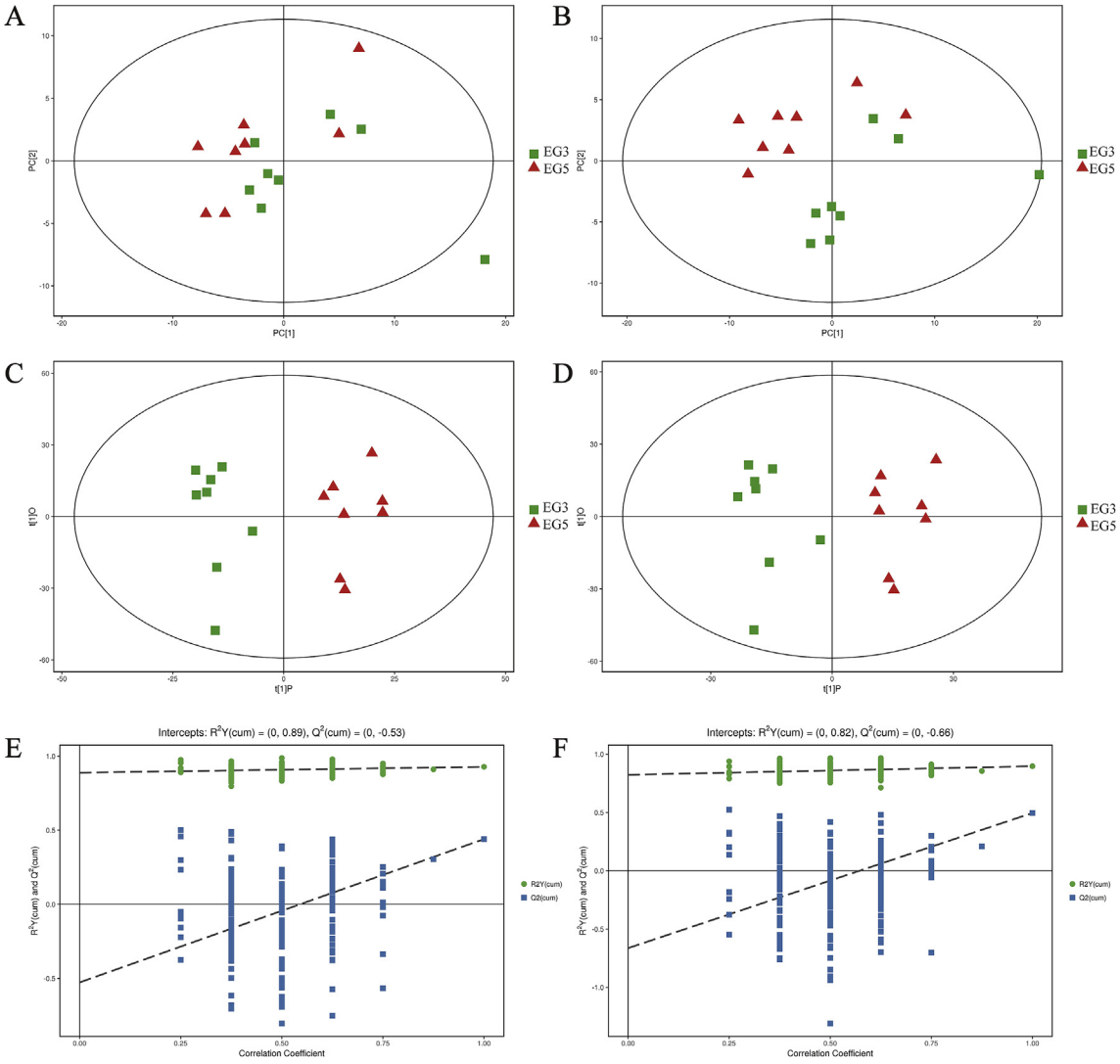

Fig. 2. PCA model score scatter plot, OPLS–DA model, and permutation test for groups EG5 and EG3. The PCA model (A and B), OPLS–DA model (C and D), and permutation test of the OPLS–DA model (E and F) were derived from the UHPLC–QTOF/MS metabolomics profiles. A, C, and E were derived from the POS ion mode, and B, D, and F were derived from the NEG ion mode.

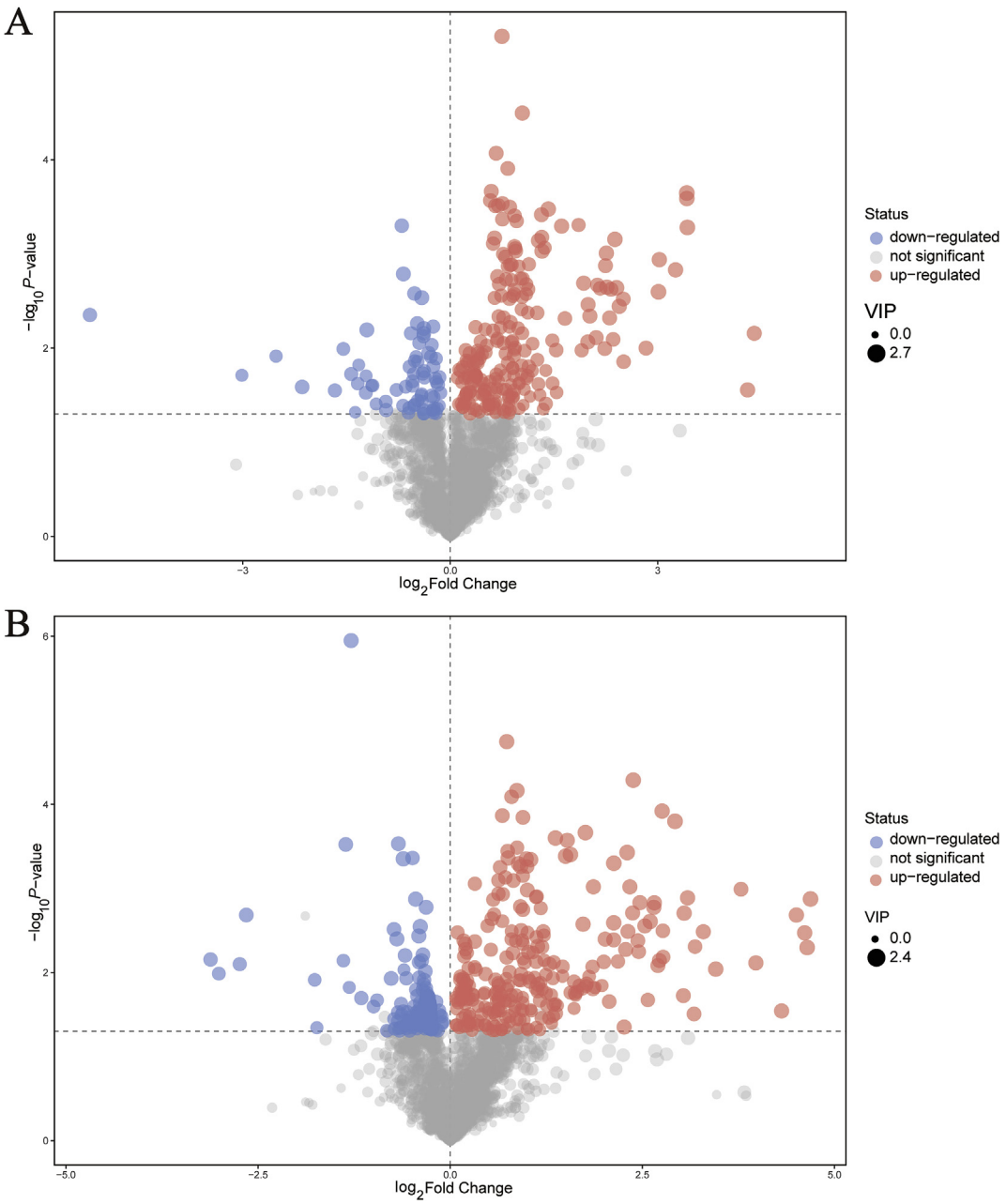

Fig. 3. Volcano plots for groups EG5 and EG3. A and B were derived from POS and NEG, respectively. In the volcano plot, each point represents a metabolite, and the point size represents the VIP value of this metabolite in the OPLS–DA model. Red, blue, and gray indicate a significantly upregulated metabolite in EG5, the opposite, and no significant difference between the two groups, respectively. (For interpretation of the references to color in this figure legend, the reader is referred to the Web version of this article.)

could be avoided by using land-based culturing, where unfortunately, food demand was high and available formulated diets for bivalves were limited. Our research team has developed optimally formulated diets for the pearl oyster *P. f. martensii* [6,25–28,31]. In this study, land-based cultured EG3 exhibited significantly higher survival rates than those cultured in natural sea. The results indicated that the living environment and external disturbances could be improved and reduced to improve the mortality of host oysters during postoperative care. Yang et al. [6] also proved that land-based culturing could enhance the survival rate of pearl oysters.

Land-based culturing can provide not only a stable environment to avoid the effects of environmental pollution and natural disasters but also supply optimal nutrients to strengthen immunity and antioxidant capacity of host oysters after transplantation and promote the maximal increase of pearl quality and yield. VD3 and its metabolite 1,25-$(OH)_2D_3$ structure is similar to the cell membrane, and when it accumulates in the cell membrane, it protects the cell membrane from free radical-induced oxidative damage [38]. Dietary VD3 has a regulating effect on the immune system of aquatic animals [7,10] and is involved in coordinating the body's antioxidant effects that influence its health [39,40]. Shellfish species lack an acquired immune system, and their defensive mechanisms mainly rely on innate immune responses [41]. ACP and AKP are both important lysosomal enzymes in marine invertebrates that could participate in nonspecific immune actions [42,43], which are involved in various metabolic processes, such as detoxification, metabolism, and biosynthesis of macromolecules, for various essential functions in living organisms [44]. Therefore, these compounds and enzymes are often used as reliable indicators in

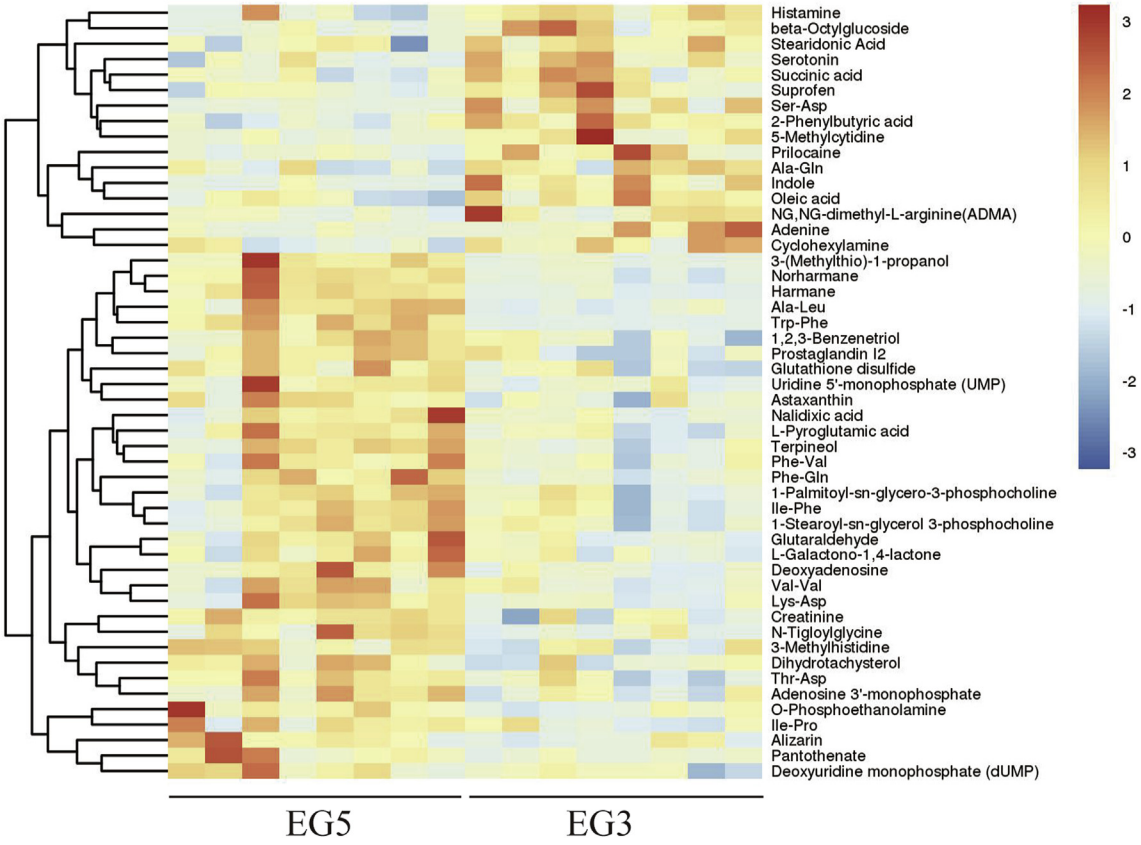

Fig. 4. Hierarchical clustering analysis on SDMs from POS. The relative metabolite level is depicted according to the color scale. Red and blue indicate upregulation and downregulation, respectively. (For interpretation of the references to color in this figure legend, the reader is referred to the Web version of this article.)

assessing the immune status of living organisms [45]. Free radicals generated by endogenous metabolic processes can cause oxidative damage that results in cell death and tissue damage [46]. Antioxidant enzymes, including CAT, SOD, and GPx, participate in primary antioxidant protection against free radicals in organisms. These enzymes are generated during immune responses and metabolic processes to prevent fatty acid oxidation, decrease toxic effects of ROS, and protect organisms from oxidative damage [26]. Bactericidal LYS is important in the nonspecific immune system against pathogenic microbes [47]. Thus, this study optimized the appropriate doses of dietary VD3 to enhance host oyster immunity through nutritional methods. Group EG3 achieved the highest activities of immune- and antioxidant-related enzymes (AKP, ACP, CAT, SOD, and LYS), which could improve the overall antioxidant and immune status. These results were consistent with previous reports on other aquatic animals [48,49]. The survival rate of group EG3 was the highest after postoperative care, thereby suggesting that the optimum levels of VD3 in the diet also increased the immunity of host oysters and reduced the mortality rate after transplantation.

However, high doses of dietary VD3 could cause different degrees of

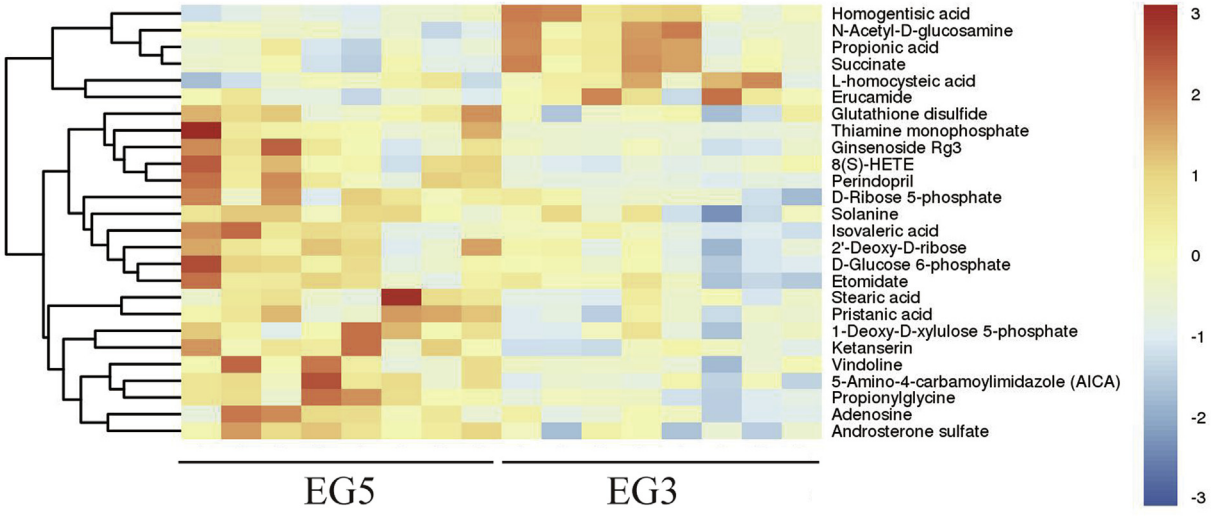

Fig. 5. Hierarchical clustering analysis on SDMs from NEG. The relative metabolite level is depicted according to the color scale. Red and blue indicate upregulation and downregulation, respectively. (For interpretation of the references to color in this figure legend, the reader is referred to the Web version of this article.)

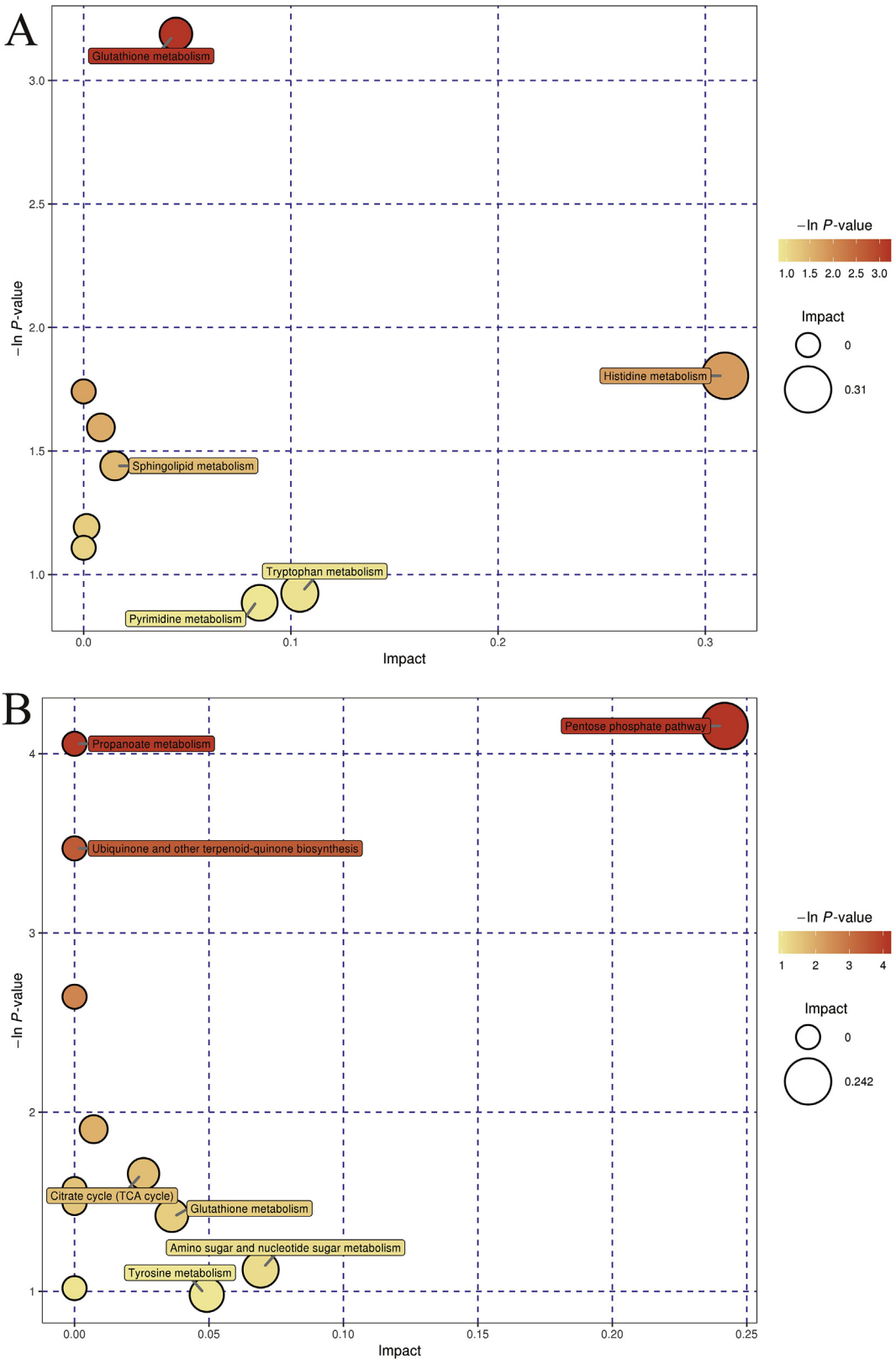

Fig. 6. Metabolome view map of significant metabolic pathways characterized in the hepatopancreas of pearl oyster *P. f. martensii* for groups EG5 and EG3. A and B are derived from POS and NEG, respectively. Significantly changed pathways based on enrichment and topology analysis are shown. The x- and y-axes represent pathway enrichment and pathway impact, respectively. Large sizes and dark colors represent major pathway enrichment and high pathway impact values, respectively. (For interpretation of the references to color in this figure legend, the reader is referred to the Web version of this article.)

structural damage to the liver of fish [10] and hepatopancreatitis of abalone [50], which could explain the decreased SOD activity in group EG5. However, the antioxidant system in the body is a complicated system. SOD is the first line of defense against oxidative damage caused by superoxide radicals in cellular antioxidant systems. When the first line of defense is destroyed, the body can launch other systems (such as the GPx system) to resist oxidative damage [50].

In this study, the high activity of GPx and concentrations of glutathione disulfide in glutathione metabolism could also prove the above surmise. Nonenzymatic small organic molecules, such as reduced glutathione, are important in maintaining the cellular redox status [51]. The pentose phosphate pathway is an alternative route of glucose catabolism that functions in NADPH formation for biosynthetic reactions [52]. In this study, pentose phosphate pathway could be activated along with high levels of D−Glucose 6−phosphate, D−Ribose 5−phosphate, and 2−Deoxy−D−ribose in group EG5, resulting in large amounts of NADPH. Glutathione reductase can use NADPH to convert glutathione disulfide into reduced glutathione, and increased production of NADPH promotes the regeneration of reduced glutathione [53]. Thus, the metabolomics analysis results suggested that pearl oysters launch GPx systems to resist oxidative damage again when VD3 was excessive.

On the other hand, lipid metabolism, including sphingolipid metabolism and arachidonic acid metabolism were influenced. Phosphatidylethanolamines are rich in readily oxidizable amino acids and docosahexaenoic acid, and phosphatidylethanolamine-derived unsaturated fatty acids usually serve as the substrate of sphingolipid peroxidation under stress [54]. Thus, the upregulation of O−phosphoethanolamine was a precursor of phosphatidylethanolamine that reflected the occurrence of sphingolipid metabolism in group EG5. Organisms could also mobilize sphingolipid to signal the control of stress response [55]. Some prostaglandins have been reported to be involved in inflammatory responses in several fish species [56]. Prostaglandin I2 is produced from arachidonic acid by a series of reactions and finally produced from prostaglandin H2 by the action of the enzyme prostacyclin synthase [57]. Transcriptomic data of our research team showed that prostaglandin E synthase-related genes were downregulated after transplantation (unpublished data). Wang et al. [58] also reported that prostaglandin E synthase was downregulated in the stress response of pearl oysters to nucleus implantation by iTRAQ-based proteomic analysis. This study indicated that the prostaglandin I2 content in group EG3 was lower than that in group EG5, thereby reflecting the occurrence of arachidonic acid metabolism and suggesting that pearl oysters in group EG5 consumed more arachidonic acid in response to stress generated from excessive VD3.

5. Conclusions

This study aimed to determine the effect of dietary VD3 levels on immunity and antioxidant capacity of the pearl oyster *P. f. martensii* after implantation. The results of this investigation showed that appropriate doses of VD3 increased the immunity and antioxidant capacity of pearl oysters. In addition, LC–MS-based metabolomics was conducted to evaluate high doses of VD3 on *P. f. martensii*. Metabolomics-based profiling of pearl oysters fed with high levels of dietary VD3 and optimum levels of dietary VD3 revealed 76 SDMs. Pathway analysis indicated that SDMs were involved in 21 pathways. Furthermore, integrated key metabolic pathway analysis suggested that pearl oysters regulated pentose phosphate pathway, glutathione metabolism, sphingolipid metabolism, and arachidonic acid metabolism in response to stress generated from excessive VD3. These findings provided a theoretical basis on understanding the effect of high doses of VD3 on pearl oysters. Therefore, the findings of this study strengthen future development and application of VD3 in the aquaculture of pearl oyster (*P. f. martensii*).

Acknowledgements

This work was supported by “Innovation Team Project” (Grant number: 2017KCXTD016) from the Department of Education of Guangdong Province, the Science and Technology Department, Guangdong Province (Grant number: 2018A030310666 and 2014A020208122), and the National Natural Science Foundation of China (Grant numbers: 31672626). LC-MS analysis was assisted by Biotree Biotech Co., Ltd. (Shanghai, China).

Appendix A. Supplementary data

Supplementary data to this article can be found online at https://doi.org/10.1016/j.fsi.2019.09.017.

References

[1] P.C. Southgate, J.S. Lucas, The Pearl Oyster, Elsevier, Oxford, 2008.
[2] P. Kishore, P.C. Southgate, A detailed description of pearl-sac development in the black-lip pearl oyster, *Pinctada margaritifera* (Linnaeus 1758), Aquacult. Res. 47 (2016) 2215–2226.
[3] T. Atsumi, T. Ishikawa, N. Inoue, R. Ishibashi, H. Aoki, H. Abe, N. Kamiya, A. Komaru, Post-operative care of implanted pearl oysters *Pinctada fucata* in low salinity seawater improves the quality of pearls, Aquaculture 422–423 (2014) 232–238.
[4] K.W. Xing, D.H. Yu, G.J. Huang, Impact of traditional Chinese medicines on recuperation of nucleus inserting cut and pearl quality, Mar. Sci. 35 (2011) 25–29 (in Chinese with English abstract).
[5] S. Fu, B.S. Huang, Y.W. Deng, F.L. Liang, The analysis on factors affecting pearl production of pearl oyster *Pinctada martensii*, J. Guangdong Ocean Univ. 33 (2013) 28–32 (in Chinese with English abstract).
[6] C.Y. Yang, Q.H. Wang, R.J. Hao, Y.S. Liao, X.D. Du, Y.W. Deng, Effects of replacing microalgae with an artificial diet on pearl production traits and mineralization-related gene expression in pearl oyster *Pinctada fucata martensii*, Aquacult. Res. 48 (2017) 5331–5337.
[7] R. Cerezuela, A.J. Cuesta, E.M. Angeles, Effects of dietary vitamin D3 administration on innate immune parameters of seabream (*Sparus aurata* L.), Fish Shellfish Immunol. 26 (2009) 243–248.
[8] K.S. Mai, Aquaculture Nutrition and Feed, China Agricuture Press, Beijing, 2015.
[9] B.W. Hollis, C.L. Wagner, Assessment of dietary vitamin D requirements during pregnancy and lactation, Am. J. Clin. Nutr. 79 (2004) 717–726.
[10] L.H. Miao, J. Xie, X.P. Ge, K.B. Wang, J. Zhu, B. Liu, M.C. Ren, Q.L. Zhou, L.K. Pan, Chronic stress effects of high doses of vitamin D3 on *Megalobrama amblycephala*, Fish Shellfish Immunol. 47 (2015) 205–213.
[11] J.K. Nicholson, J.C. Lindon, Systems biology: metabonomics, Nature 455 (2008) 1054–1056.
[12] R.J. Hao, Z.M. Wang, C.Y. Yang, Y.W. Deng, Z. Zheng, Q.H. Wang, X.D. Du, Metabolomic responses of juvenile pearl oyster *Pinctada maxima* to different growth performances, Aquaculture 491 (2018) 258–265.
[13] R.J. Hao, X.D. Du, C.Y. Yang, Y.W. Deng, Z. Zheng, Q.H. Wang, Integrated application of transcriptomics and metabolomics provides insights into unsynchronized growth in pearl oyster *Pinctada fucata martensii*, Sci. Total Environ. 666 (2019) 46–56.
[14] R. Grandiosa, F. Mérien, T. Young, T.V. Nguyen, N. Gutierrez, E. Kitundu, A.C. Alfaro, Multi-strain probiotics enhance immune responsiveness and alters metabolic profiles in the New Zealand black-footed abalone (*Haliotis iris*), Fish Shellfish Immunol. 82 (2018) 330–338.
[15] C. Xu, X.D. Wang, F.L. Han, C.L. Qi, E.C. Li, J.L. Guo, J.G. Qin, L.Q. Chen, α-lipoic acid regulate growth, antioxidant status and lipid metabolism of Chinese mitten crab *Eriocheir sinensis*: optimum supplement level and metabonomics response, Aquaculture 506 (2019) 94–103.
[16] M.X. Ning, P.P. Wei, H. Shen, X.H. Wan, M.J. Jin, X.Q. Li, H. Shi, Y. Qiao, G. Jiang, W. Gu, W. Wang, L. Wang, Q.G. Meng, Proteomic and metabolomic responses in hepatopancreas of whiteleg shrimp *Litopenaeus vannamei* infected by microsporidian *Enterocytozoon hepatopenaei*, Fish Shellfish Immunol. 87 (2019) 534–545.
[17] T. Cappello, M. Maisano, A. Mauceri, S. Fasulo, ^{1}H NMR-based metabolomics investigation on the effects of petrochemical contamination in posterior adductor muscles of caged mussel *Mytilus galloprovincialis*, Ecotoxicol. Environ. Saf. 142 (2017) 417–422.
[18] T.G. Huynh, A.C. Cheng, C.C. Chi, K.H. Chiu, C.H. Liu, A synbiotic improves the immunity of white shrimp, *Litopenaeus vannamei*: metabolomic analysis reveal compelling evidence, Fish Shellfish Immunol. 79 (2018) 284–293.
[19] W. Tuffnail, G.A. Mills, P. Cary, R. Greenwood, An environmental ^{1} H NMR metabolomic study of the exposure of the marine mussel *Mytilus edulis* to atrazine, lindane, hypoxia and starvation, Metabolomics 5 (2009) 33–43.
[20] B.L. Baumgarner, B.R. Cooper, Evaluation of a tandem gas chromatography/time-of-flight mass spectrometry metabolomics platform as a single method to investigate the effect of starvation on whole-animal metabolism in rainbow trout (*Oncorhynchus mykiss*), J. Exp. Biol. 215 (2012) 1627–1632.
[21] L. Wagner, S. Trattner, J. Pickova, P. Gómez-Requeni, A.A. Moazzami, ^{1}H NMR-

based metabolomics studies on the effect of sesamin in Atlantic salmon (*Salmo salar*), Food Chem. 147 (2014) 98–105.
[22] Y. Jin, L.X. Tian, S.W. Xie, D.Q. Guo, H.J. Yang, G.Y. Liang, Y.J. Liu, Interactions between dietary protein levels, growth performance, feed utilization, gene expression and metabolic products in juvenile grass carp (*Ctenopharyngodon idella*), Aquaculture 437 (2015) 75–83.
[23] J. Xu, F. Wang, I. Jakovlić, W. Prisingkorn, J.T. Li, W.M. Wang, Y.H. Zhao, Metabolite and gene expression profiles suggest a putative mechanism through which high dietary carbohydrates reduce the content of hepatic betaine in *Megalobrama amblycephala*, Metabolomics 14 (2018) 94.
[24] Q.Q. Ma, Q. Chen, Z.H. Shen, D.L. Li, T. Han, J.G. Qin, L.Q. Chen, Z.Y. Du, The metabolomics responses of Chinese mitten-hand crab (*Eriocheir sinensis*) to different dietary oils, Aquaculture 479 (2017) 188–199.
[25] C.Y. Yang, R.J. Hao, X.D. Du, Q.H. Wang, Y.W. Deng, R.J. Sun, Z. Zheng, GC-TOF/MS-based metabolomics studies on the effect of protein sources in formulated diet for pearl oyster *Pinctada fucata martensii*, Aquaculture 486 (2018) 139–147.
[26] C.Y. Yang, R.J. Hao, Y.W. Deng, Y.S. Liao, Q.H. Wang, R.J. Sun, Y. Jiao, X.D. Du, Effects of protein sources on growth, immunity and antioxidant capacity of juvenile pearl oyster *Pinctada fucata martensii*, Fish Shellfish Immunol. 67 (2017) 411–418.
[27] C.Y. Yang, R.J. Hao, X.D. Du, Y.W. Deng, R.J. Sun, Q.H. Wang, Metabolomics responses of pearl oysters (*Pinctada fucata martensii*) fed a formulated diet indoors and cultured with natural diet outdoors, Front. Physiol. 9 (2018) 944.
[28] C.Y. Yang, R.J. Hao, X.D. Du, Q.H. Wang, Y.W. Deng, R.J. Sun, Response to different dietary carbohydrate and protein levels of pearl oysters (*Pinctada fucata martensii*) as revealed by GC-TOF/MS-based metabolomics, Sci. Total Environ. 650 (2019) 2614–2623.
[29] X.D. Du, Y.W. Deng, Q.H. Wang, S.H. Xie, D. Liu, Haixuan No 1 stock of pearl oyster *Pinctada martensii*, China Fish. 10 (2015) 53–55.
[30] X. Zhan, Z.F. Gu, C.C. Yu, H.Y. Wen, Y.H. Shi, A.M. Wang, Expressed sequence tags 454 sequencing and biomineralization gene expression for pearl sac of the pearl oyster, *Pinctada fucata martensii*, Aquacult. Res. 46 (2015) 745–758.
[31] Q.H. Wang, C.Y. Yang, X.D. Du, X.W. Liu, R.J. Sun, Y.W. Deng, Growth performance and biochemical composition of juvenile pearl oyster *Pinctada martensii* fed on artificial diets, Aquacult. Int. 24 (2016) 995–1005.
[32] C.A. Smith, E.J. Want, G. O'Maille, R. Abagyan, G. Siuzdak, XCMS: processing mass spectrometry data for metabolite profiling using nonlinear peak alignment, matching, and identification, Anal. Chem. 78 (2006) 779–787.
[33] C. Kuhl, R. Tautenhahn, C. Böttcher, T.R. Larson, S. Neumann, CAMERA: an integrated strategy for compound spectra extraction and annotation of liquid chromatography/mass spectrometry data sets, Anal. Chem. 84 (2012) 283–289.
[34] E. Saccenti, H.C.J. Hoefsloot, A.K. Smilde, J.A. Westerhuis, M.M.W.B. Hendriks, Reflections on univariate and multivariate analysis of metabolomics data, Metabolomics 10 (2014) 361–374.
[35] O. Latchere, G. Le Moullac, N. Gaertner-Mazouni, J. Fievet, K. Magré, D. Saulnier, Influence of preoperative food and temperature conditions on pearl biogenesis in *Pinctada margaritifera*, Aquaculture 479 (2017) 176–187.
[36] J.H. Li, C.Y. Yang, Q.H. Wang, X.D. Du, Y.W. Deng, Growth and survival of host pearl oyster *Pinctada fucata martensii* (Dunker, 1880) treated by different biofouling-clean methods in China, Estuar. Coast Shelf Sci. 207 (2018) 104–108.
[37] L. Adzigbli, R.J. Hao, Y. Jiao, Y.W. Deng, X.D. Du, Q.H. Wang, R.L. Huang, Immune response of pearl oysters to stress and diseases, Rev. Aquac. doi: 10.1111/raq.12329.
[38] H. Wiseman, Vitamin D is a membrane antioxidant Ability to inhibit iron-dependent lipid peroxidation in liposomes compared to cholesterol, ergosterol and tamoxifen and relevance to anticancer action, FEBS Lett. 1–3 (1993) 285–288.
[39] R.M. Martinez-Alvarez, A.E. Morales, A. Sanz, Antioxidant defenses in fish: biotic and abiotic factors, Rev. Fish Biol. Fish. 1–2 (2005) 75–88.
[40] E.J. Lock, R. Waagbø, S.W. Bonga, G. Flik, The significance of vitamin D for fish: a review, Aquacult. Nutr. 16 (2010) 100–116.
[41] F.J. Jiang, X. Yue, H.X. Wang, B.Z. Liu, Transcriptome profiles of the clam *Meretrix petechialis* hepatopancreas in response to *Vibrio* infection, Fish Shellfish Immunol. 62 (2017) 175–183.
[42] M.F. Rahmana, M.K.J. Siddiqui, Biochemical effects of vepacide (from *Azadirachta indica*) on Wistar rats during subchronic exposure, Ecotoxicol. Environ. Saf. 59 (2004) 332–339.
[43] S. Liang, X. Luo, W.W. You, L.Z. Luo, C.H. Ke, The role of hybridization in improving the immune response and thermal tolerance of abalone, Fish Shellfish Immunol. 39 (2014) 69–77.
[44] T. Suzuki, K. Mori, Hemolymph lectin of the pearl oyster, *Pinctada fucata martensii*: a possible non-self recognition system, Dev. Comp. Immunol. 14 (1990) 161–173.
[45] Y.X. Ma, Z.M. Liu, Z.P. Yang, M. Li, J. Liu, J. Song, Effects of dietary live yeast *Hanseniaspora opuntiae* C21 on the immune and disease resistance against *Vibrio splendidus* infection in juvenile sea cucumber *Apostichopus japonicus*, Fish Shellfish Immunol. 34 (2013) 66–73.
[46] J. Kehrer, Free radicals as mediators of tissue injury and disease, Crit. Rev. Toxicol. 23 (1993) 21–48.
[47] Y.F. Duan, Y. Wang, Q.S. Liu, J.S. Zhang, D.L. Xiong, Changes in the intestine barrier function of *Litopenaeus vannamei* in response to pH stress, Fish Shellfish Immunol. 88 (2019) 142–149.
[48] M.M. Duan, C.F. Wang, C.X. Xie, Effects of dietary vitamin D3 on antioxidant and immune capacity of juvenile *Pelteobagrus fulvidraco*, Freshw. Fish. 34 (2015) 80–84 (in Chinese with English abstract).
[49] L.L. Wang, B.S. Li, J.Y. Wang, Y.Z. Sun, X.J. Han, Y.P. Wang, T.T. Hao, S.X. Wang, Effects of dietary vitamin D3 on growth performance, body composition, and antioxidant capacity of the juvenile sea cucumber, Progress in Fishery Sciences 40 (2019) 110–118 (in Chinese with English abstract).
[50] J.H. Fu, W.B. Zhang, K.S. Mai, X.N. Feng, W. Xu, F.Z.G. Liu, Effect of dietary vitamin D on growth and antioxidant responses of abalone *Haliotis discus hannai* Ino, Chin. High. Technol. Lett. 16 (2006) 1306–1311 (in Chinese with English abstract).
[51] B. Wen, S.R. Jin, Z.Z. Chen, J.Z. Gao, Physiological responses to cold stress in the gills of discus fish (*Symphysodon aequifasciatus*) revealed by conventional biochemical assays and GC-TOF-MS metabolomics, Sci. Total Environ. 640–641 (2018) 1372–1381.
[52] A. Moreira, E. Figueira, A.M.V.M. Soares, R. Freitas, The effects of arsenic and seawater acidification on antioxidant and biomineralization responses in two closely related *Crassostrea* species, Sci. Total Environ. 545–546 (2016) 569–581.
[53] J. Fan, J. Ye, J.J. Kamphorst, T. Shlomi, C.B. Thompson, J.D. Rabinowitz, Quantitative flux analysis reveals folate-dependent NADPH production, Nature 510 (2014) 298.
[54] R. González-Domínguez, T. García-Barrera, J.L. Gómez-Ariza, Combination of metabolomic and phospholipid-profiling approaches for the study of Alzheimer's disease, J. Proteomics 104 (2014) 37–47.
[55] H.P. Hrobuchak, A.P. Ardasheva, D.P. Servello, A.P. Nolan, J.P. Chan, The role of the sphingolipid metabolism pathway in healthy aging, FASEB J. 31 (2017) 935.4.
[56] V.G.V. Gomez-Abellan, M.S.M.P. Sepulcre, The role of prostaglandins in the regulation of fish immunity, Mol. Immunol. 69 (2016) 139–145.
[57] A. Kats, T. Båge, P. Georgsson, J. Jönsson, H.C. Quezada, A. Gustafsson, L. Jansson, C. Lindberg, K. Näsström, T. Yucel-Lindberg, Inhibition of microsomal prostaglandin E synthase-1 by aminothiazoles decreases prostaglandin E2 synthesis in vitro and ameliorates experimental periodontitis in vivo, FASEB J. 27 (2013) 2328–2341.
[58] W. Wang, Q.N. Lei, H.Y. Liang, J.J. He, Towards a better understanding of allograft-induced stress response in the pearl oyster *Pinctada fucata martensii*: insights from iTRAQ-based comparative proteomic analysis, Fish Shellfish Immunol. 86 (2019) 186–195.